INTERNATIONAL DESIGN CONFERENCE - DESIGN 2002
Dubrovnik, May 14 - 17, 2002.

DYNAMICS OF MOTORCYCLE USING FLEXIBLE ELEMENTS

Salvatore Massimo Oliveri, Michele Calì and Leonardo Catalano

Keywords: Dynamics, Motorcycle, Flexible bodies, F.E.M.

1. Introduction

Motorcycle dynamics are greatly influenced by the torsional and flexural stiffness of the frame, above all during movement along curvilinear trajectories. In previous papers, the authors developed mathematical models constructed with solely rigid bodies to simulate the dynamic behaviour the motor vehicle. Here, the study is extended to take advantage of the possibility of employing flexible elements to simulate the frame.
Rigid frame models, already little suited for investigations into comfort, are clearly limited when studying the handling of the motorcycle. It is in fact known that motorcycle performance, particularly in the case of competition models, is strongly conditioned by the flexibility of the frame carrying the suspension and propulsion units, which in some cases contribute to the stiffness of the frame itself. It is also known that precisely this flexibility of the frame is used to improve vehicle dynamics, favouring or contrasting gyroscopic effects.
The present study describes the synergetic combination of the MDI/ADAMS and MSC/VisualNastran calculation programs to construct the three-dimensional multibody model of a high performance motorcycle, complete with suspension units, motor-propulsion system and rider, with a frame of flexible elements.

2. Construction of the model

The three-dimensional model of the motorcycle was constructed using the MDI/ADAMS calculation code. Through the use of multibody systems, consisting of an assembly of parts connected by junctions, constraints and forces, the program makes it possible to simulate the motorcycle's kinematic and dynamic behaviour and to study some characteristic aspects. As the motorcycle is a labile system, in order to simulate its real behaviour, both when travelling along a straight and when rounding a given curve, it is necessary to apply a feed-back control system, developed by the authors in a previous study.
The MCAD model of the lattice frame was constructed using a parametric modeller, based on two-dimensional blueprints and measurements made on the real motorcycle using reverse engineering techniques.
The geometry supporting the construction of the FEM model is made up of NURBS surfaces, situated close to the mid-surface of the tubular beams. This schematisation lends itself to the topological optimisation of the frame, based on linear calculations of the stresses and strains directed at identifying the optimal characteristic dimensions of the cross-sections.
After schematising the frame as a super-element, free-body modal analysis was performed, indicating the points of application of forces for the multibody analysis as independent nodes of rigid elements (RBE2) connected to the elements making up the frame structure.

Figure 1 shows the geometry of the frame and its discretisation, while the characteristic data of the material and the FEM model, constructed using shell elements with four and three nodes (CQUAD4 and CTRIA3: the latter less than 3% of the total number of elements) are reported in Table 1.

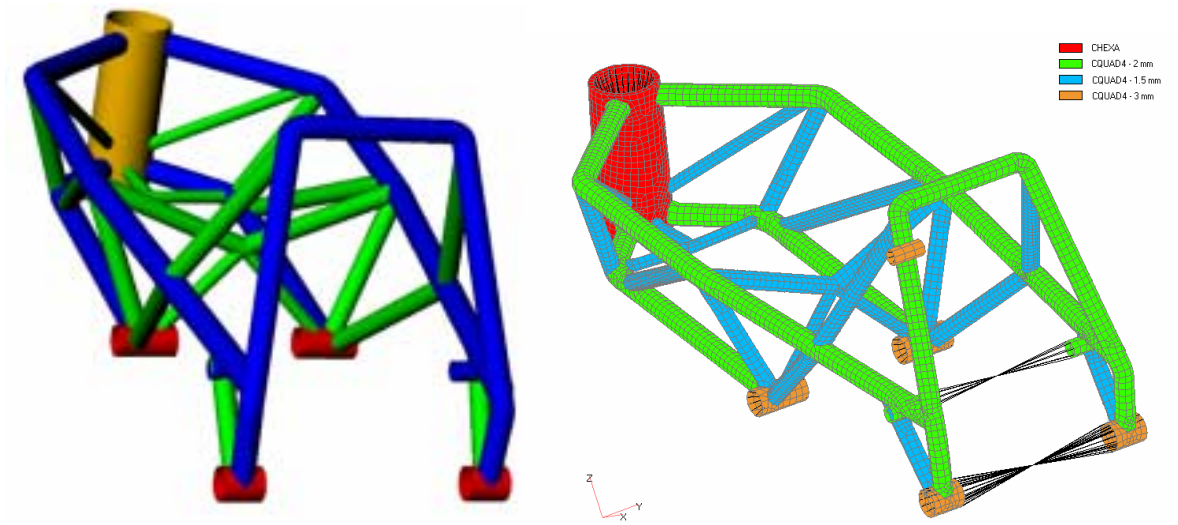

Figure 1. Geometry of frame and FEM model

In the motorcycle under examination the frame consists of a lattice of AlSi 450 steel (Fig 1), inside which the engine is suspended from six anchorage points. The rear fork connecting pin is also inserted into the lower attachment holes, thus allowing its rotation about its own axis. In this configuration the engine is an element stiffening the frame making it necessary to determine its mass and inertia.

Table 1. Characteristics of material and FEM model

Nodes	12427	**Material**	AlSi 450
Elements	11879	**Lengthening (A)**	20%
		Fracture stress (R)	480 daN/mm^2

The spring-shock absorber units consist of two masses and two single component forces which schematise the stiffness and damping characteristics of the real systems interacting with the frame. Adopting spline elements it was possible to duplicate these two characteristics in a non-linear way. The scheme of the rear suspension, of quadrilateral oscillating arm type, is shown in Figure 2, where the upper rocker arm can be seen connected to the frame by a constraining revolute joint placed outside the mid-plane of motorcycle, to which the spring-shock absorber unit and reaction strut are attached.

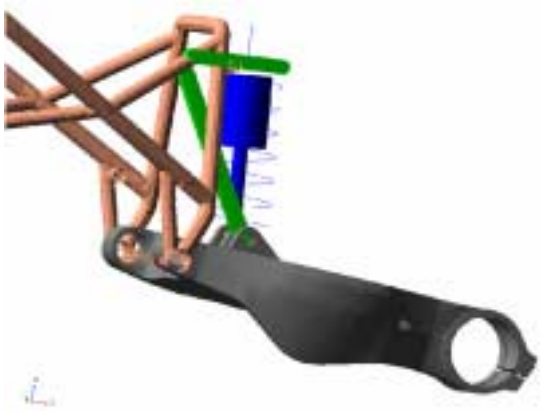

Figure 2. Model of rear suspension

To calculate the exact value of the polar moments of inertia of the wheels complete with accessories, reported with the values of mass supplied by the manufacturer in Table 2, it was necessary to construct MCAD models.

Table 2. Inertial characteristics of wheels

Front wheel		Rear wheel	
Mass	12 kg	Mass	14 kg
Moment of inertia	0.5 kg m^2	Moment of inertia	0.7 kg m^2

The wheels were modelled with particular accuracy due to the fact that they have a predominant influence on the dynamics of the motorcycle. In fact, their moment of inertia effects both acceleration and braking, the gyroscopic effect determines the stability of the motorcycle and, as suspended masses, they contribute to the correct function of the suspension units.
Both handling and comfort, therefore, are influenced by the mass of the wheels and by their geometric configuration. Also the tyre was modelled using an assembly of parts, forces and graphical elements which serve to reproduce the mechanics of the tyre-road surface contact. The model adopted allows the phenomenon of longitudinal slip to be correlated with lateral slip, and allows simulations with maximum roll angles of 35°, a value commonly reached by high performance motorcycles when rounding curves.
The multibody model of the motorcycle was then obtained by assembling the parts: flexible frame, rider, motor-propulsion system, a pair of silencers, fuel tank, seat connected to supporting sub-frame, instrument-head light unit, two handle bars, two footrests, rear suspension unit complete with fork, front fork arms, front wheel, rear wheel, and the fairing, for a total of 26 parts.
The total mass is 190 kg, with a distribution of 51% to the front and 49% to the rear, as in the real motorcycle. The model has 45 degrees of freedom.
Since the rider has mass and inertia characteristics similar to those of the motorcycle, he has a fundamental importance in the statics and dynamics of the vehicle. The rider has a mass of 75 kg and is composed of 13 rigid parts linked by bushings with elevated stiffness, and connected to the motorcycle by five bushings that constrain his hands to the handlebars, trunk to the saddle and lower limbs to the footrests. In this way the rider's mass is distributed on the seat and footrests under static conditions and also on the handlebars under dynamic conditions. The rider can be made to assume any position, but in this study a hunched position (usual for the motorcycle under examination) was chosen for all simulations in order to avoid excessive complication of the calculation.
The graphical appearance of the model (Figure 3) was rendered with elevated precision to render the dynamic simulations as clear as possible, making the physical phenomenon easier to understand and any macroscopic kinematic anomalies more immediately apparent.

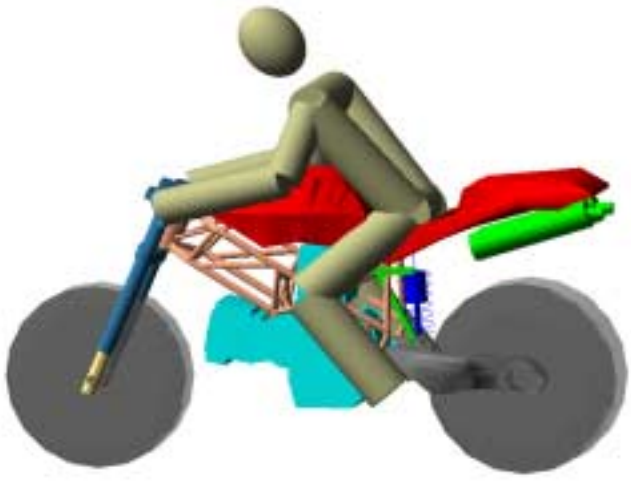

Figure 3. Motorcycle without fairing

2.1 Validation of the frame

The flexible frame characterises the model developed in this study. It was therefore necessary to validate the model through a comparison with data obtained experimentally. With this aim, the torsional stiffness was calculated, simulating the experimental measurements made by the manufacturer. For this, the frame is constrained at the engine attachment points and a known force is applied to the steering column sleeve using a steel bar. The sleeve itself is rigidly constrained by a second bar so that the rotation can be measured exactly during the application of the load, without this being influenced by the deformation of the loading bar itself. The calculated torsional stiffness value is congruent with the mean experimentally measured value.

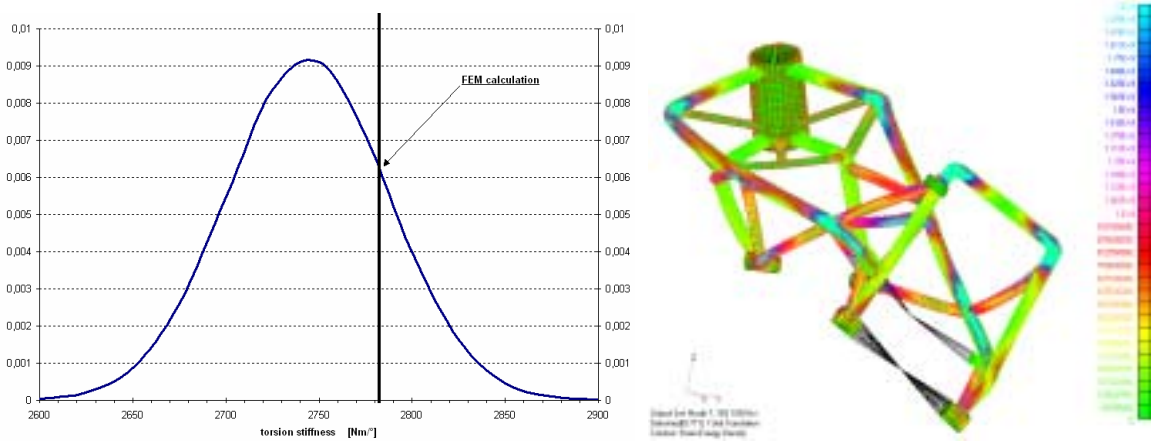

Figure 4. Torsional stiffness of the motorcycle frame

Figure 4 shows the form of the expected normal distribution, while the values in question and the standard deviation, the value which guarantees the validity of the model, are reported in Table 4.

Table 4. Torsional stiffness of motorcycle frame

	Torsional stiffness (Nm/°)	Standard deviation
$M_{calculated}$	2783	
$M_{tmeasured}$	2744.083333	43.41440551

3. Analysis

With the aim of evidencing the different dynamic behaviour of the model when a frame composed of flexible elements is used, two typical manoeuvres characterising the comfort and handling of the motorcycle were simulated. After having implemented the feed-back control system, therefore, two manoeuvres were simulated with the motorcycle in road trim: passage over an irregularity in the road (in the form of a sinusoidal hump 30 mm high and 3000 mm long) at a constant velocity of about 40 km/h; and then travelling along a demanding “S” bend trajectory with a minimum radius of curvature of 20 m.

Both analyses were repeated four times with four different typologies of frame inertia calculation.

In the program used, the flexible body equation is:

$$\mathbf{M}\ddot{\boldsymbol{\xi}} + \dot{\mathbf{M}}\dot{\boldsymbol{\xi}} - \frac{1}{2}\left[\frac{\partial \mathbf{M}}{\partial \boldsymbol{\xi}}\dot{\boldsymbol{\xi}}\right]^{T}\dot{\boldsymbol{\xi}} + \mathbf{K}\boldsymbol{\xi} + \mathbf{f}_{g} + \mathbf{D}\dot{\boldsymbol{\xi}} + \left[\frac{\partial \boldsymbol{\Psi}}{\partial \boldsymbol{\xi}}\right]^{T}\boldsymbol{\lambda} = \mathbf{Q} \tag{1}$$

Where M is the matrix of mass, a complex function identified by nine invariants of inertia, whose activation modifies the conditions of frame flexibility and improves the efficiency of the calculation.

$$\mathbf{M} = \begin{bmatrix} \mathbf{M}_{tt} & \mathbf{M}_{tr} & \mathbf{M}_{tm} \\ & \mathbf{M}_{rr} & \mathbf{M}_{rm} \\ \text{symmetric} & & \mathbf{M}_{mm} \end{bmatrix} \tag{2}$$

Where the various parameters are terms used in the calculation of single elements of the above matrix:

$$\begin{aligned} \mathbf{M}_{tt} &= \mathcal{I}^1\mathbf{I} & \mathbf{M}_{rr} &= \mathbf{B}^T\left[\mathcal{I}^7 - \left[\mathcal{I}_j^8 + \mathcal{I}_j^{8T}\right] q_j - \mathcal{I}_{ij}^9 q_i q_j\right]\mathbf{B} \\ \mathbf{M}_{tr} &= -\mathbf{A}\left[\mathcal{I}^2 + \widetilde{\mathcal{I}_j^3 q_j}\right]\mathbf{B} & \mathbf{M}_{rm} &= \mathbf{B}^T\left[\mathcal{I}^4 + \mathcal{I}_j^5 q_j\right] \\ \mathbf{M}_{tm} &= \mathbf{A}\mathcal{I}^3 & \mathbf{M}_{mm} &= \mathcal{I}^6 \end{aligned} \tag{3}$$

The highest level of accuracy is obtained with *Full coupling* in which all the invariants are activated. The program default is *Partial coupling* where the fifth and ninth invariants, which account for second order correction of the inertia tensor of the flexible body, are disactivated, thus sacrificing a modest level of accuracy compared to *Full coupling*. In the *Constant* model, as well as the fifth and ninth, also the third, fourth and eighth invariants are disactivated, guaranteeing an accurate response only if the flexible component is quite rigid. Finally, the inertia is calculated considering the frame completely rigid, zeroing the invariants associated with the modal terms of the mass matrix.

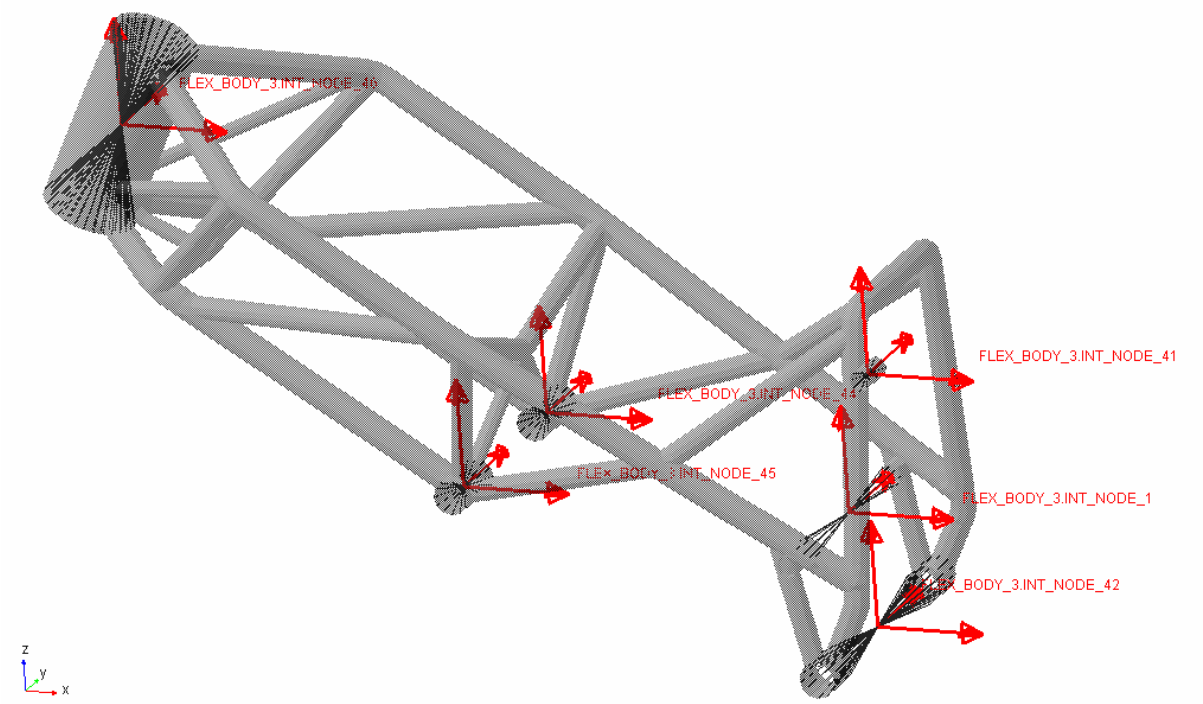

Figure 5. Marker positions and frame nodes

Figure 5 shows the position of the frame nodes and relevant markers, where actions are exchanged between the flexible body and the other rigid parts.

3.1 Passage over hump

In order to simulate the rear hub of the motorcycle, a torque was applied, with a law shown in Figure 6, calculated as a function of that measured at the engine pinion, considering the transmission ratio and subtracting the resisting couple due to the effect of the wheels.

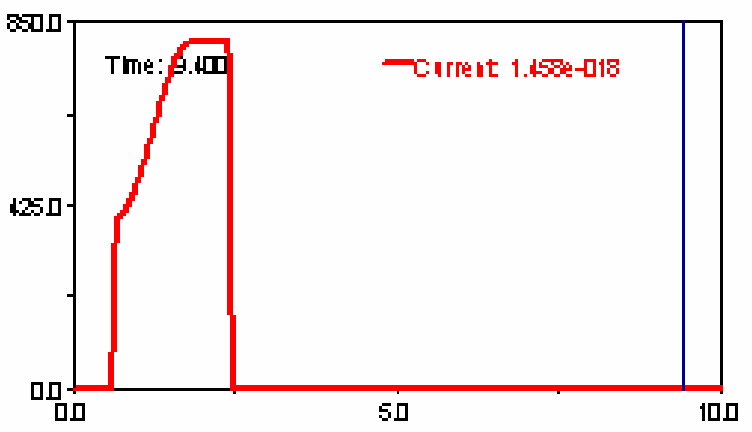

Figure 6. Torque

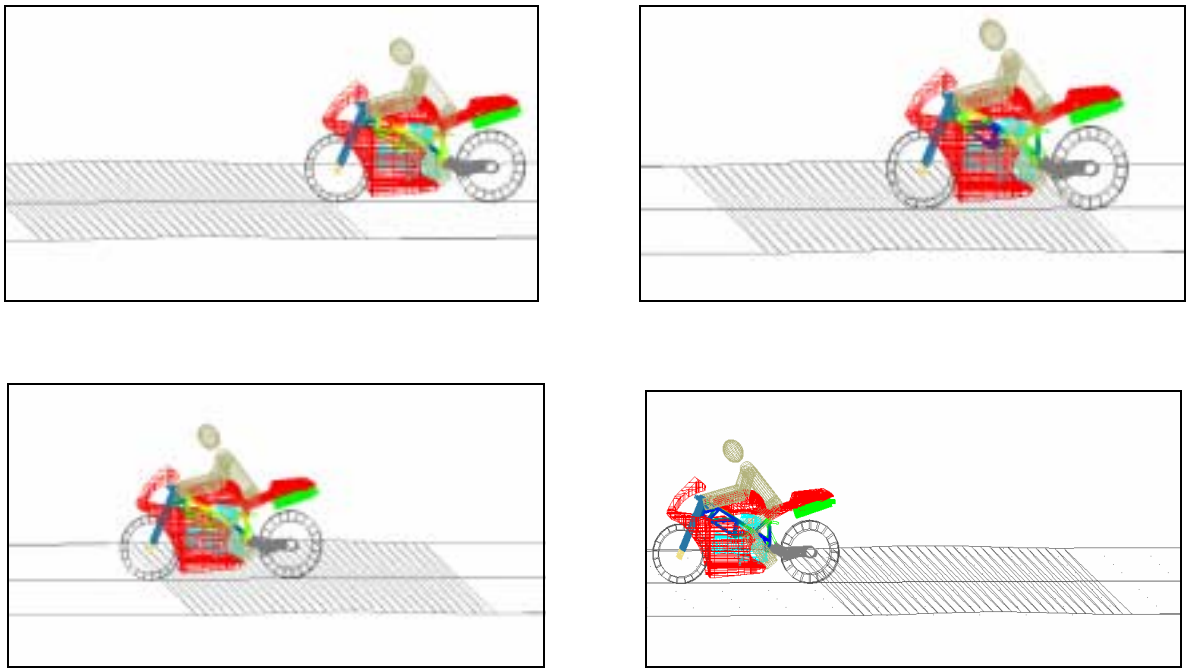

Figure 7. Passage over a sinusoidal irregularity in road surface

The front wheel mounts the hump after *6.6 s*, while the rear wheel leaves it approximately 4/10 of a second later (Figure 7).

The graph in Figure 8 shows the acceleration obtained at the barycentre of the rider's chest. The graph evidences that the values calculated considering the various typologies of flexible frame are lower than those measured with a rigid frame, but close to the real values.

Similarly, the graph shows that the *Constant* inertial configuration gives an unrealistic response, in agreement with the discussion above, since the frame is not so rigid that it can be represented by this configuration.

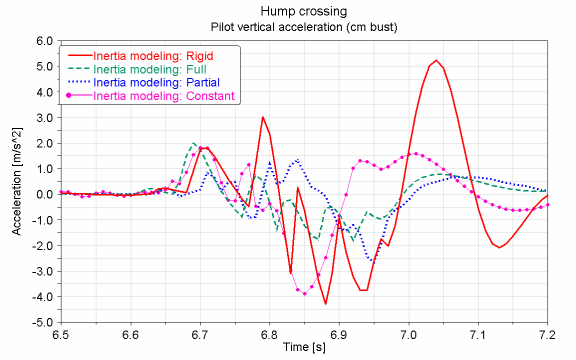

Figure 8. Vertical acceleration of rider

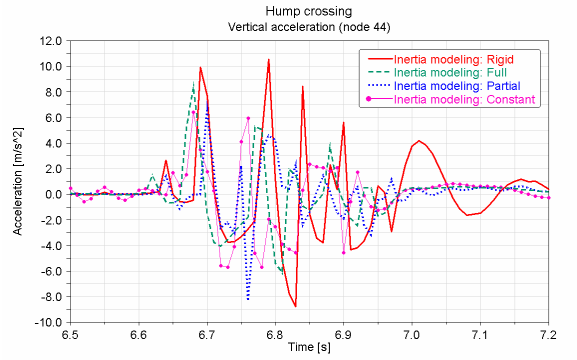

Figure 9. Vertical acceleration of engine

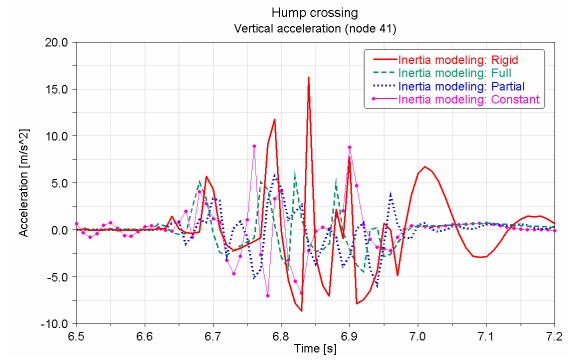

Figure 10. Vertical acceleration of rear suspension

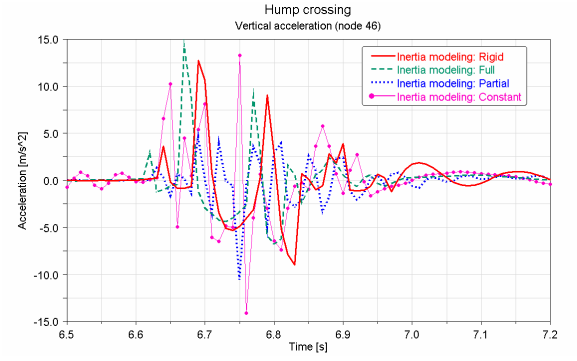

Figure 11. Vertical acceleration of steering column

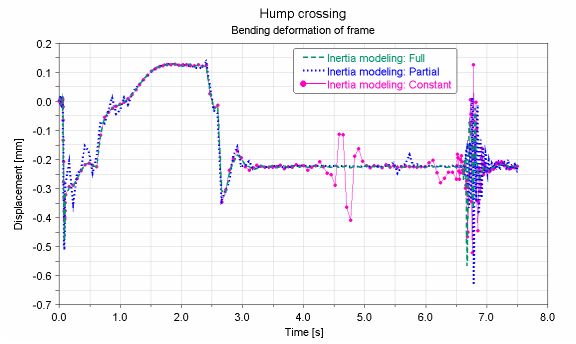

Figure 12. Flexural deformation of frame *Full* inertia configuration

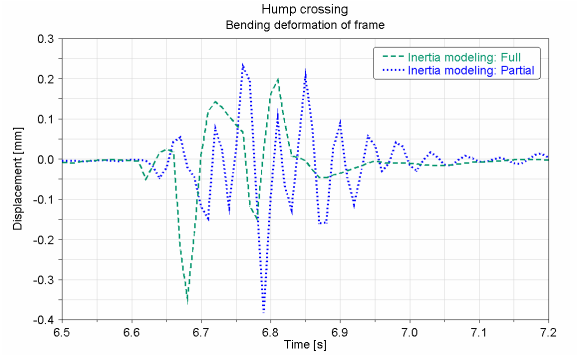

Figure 13. Flexural deformation of frame *Partial* inertia configuration

Analogous considerations can be made from the analysis of Figures 9, 10 and 11 which show the vertical components of the acceleration calculated at the points, respectively, of the front right engine attachment (node 44), the rear suspension rocker arm attachment (node 41) and in the steering column sleeve (node 46).

Figures 12 and 13 show the flexural deformation of the frame in the *Full* and *Partial* inertia configurations, measured as difference between two points located in the central zone of the steering column sleeve and the rear suspension attachment.

From $t = 0\ s$ to $t = 0.2\ s$ the deformation is fictitious since it is the result of static setting of the model, while from $t = 0.2\ s$ to $t = 3\ s$ the deformation is due to the action of the couple applied to the rear wheel, which loads the frame through the leverage of the suspension and the fork.

With regard to the trend of the flexural deformation measured during the passage over the hump, the value of 0.5 mm is compatible with the stiffness characteristics of the frame.
In conclusion, all the graphs show a different response between the flexible and rigid frame inertia configurations.

3.2 Curvilinear trajectory

The same torque law reported in Figure 6 was applied to make the motorcycle describe an “S” bend trajectory. Using a step function, the controller makes the motorcycle turn through a left bend, then a counter-curve to the right, and finally another left bend to realign on the straight trajectory (Figure 14).

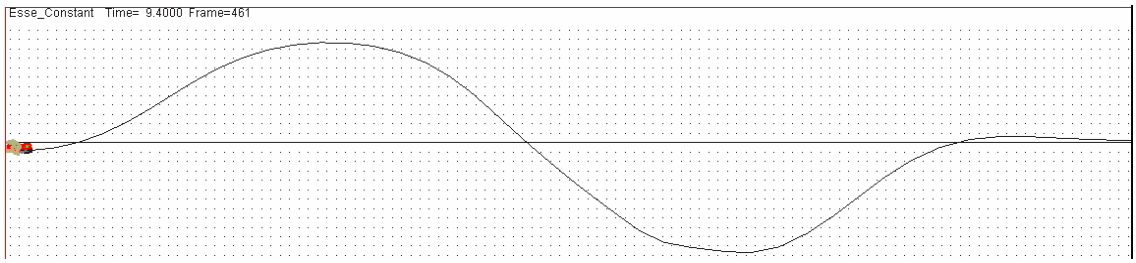

Figure 14. Curvilinear trajectory

The manoeuvre resulting in a maximum inclination of the motorcycle of 29.8° is performed at a mean velocity of 40 km/h, beginning at $t = 3.10$ *s* and finishing at $t = 10$ *s*.

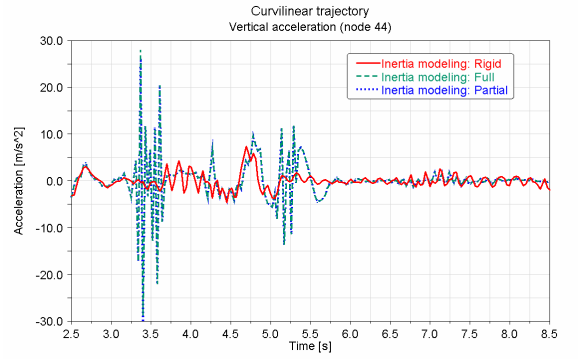

Figure 15. Vertical acceleration of engine

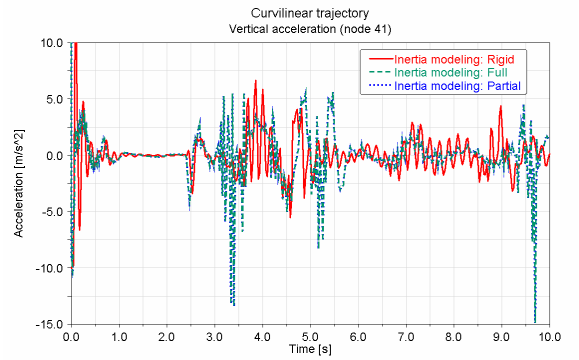

Figure 16. Vertical acceleration of rear suspension

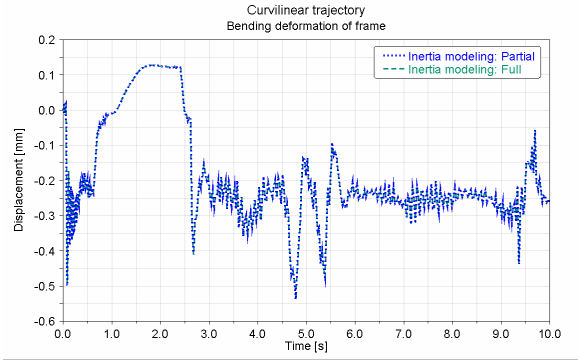

Figure 17. Flexural deformation of frame

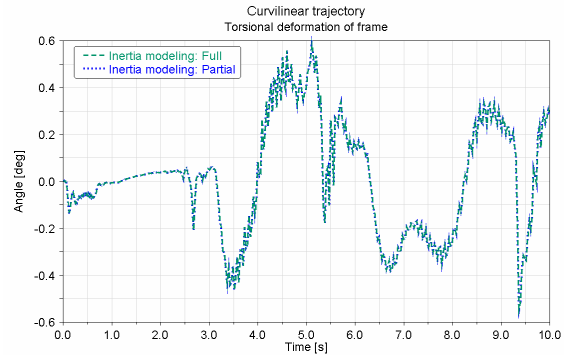

Figure 18. Torsional deformation of frame

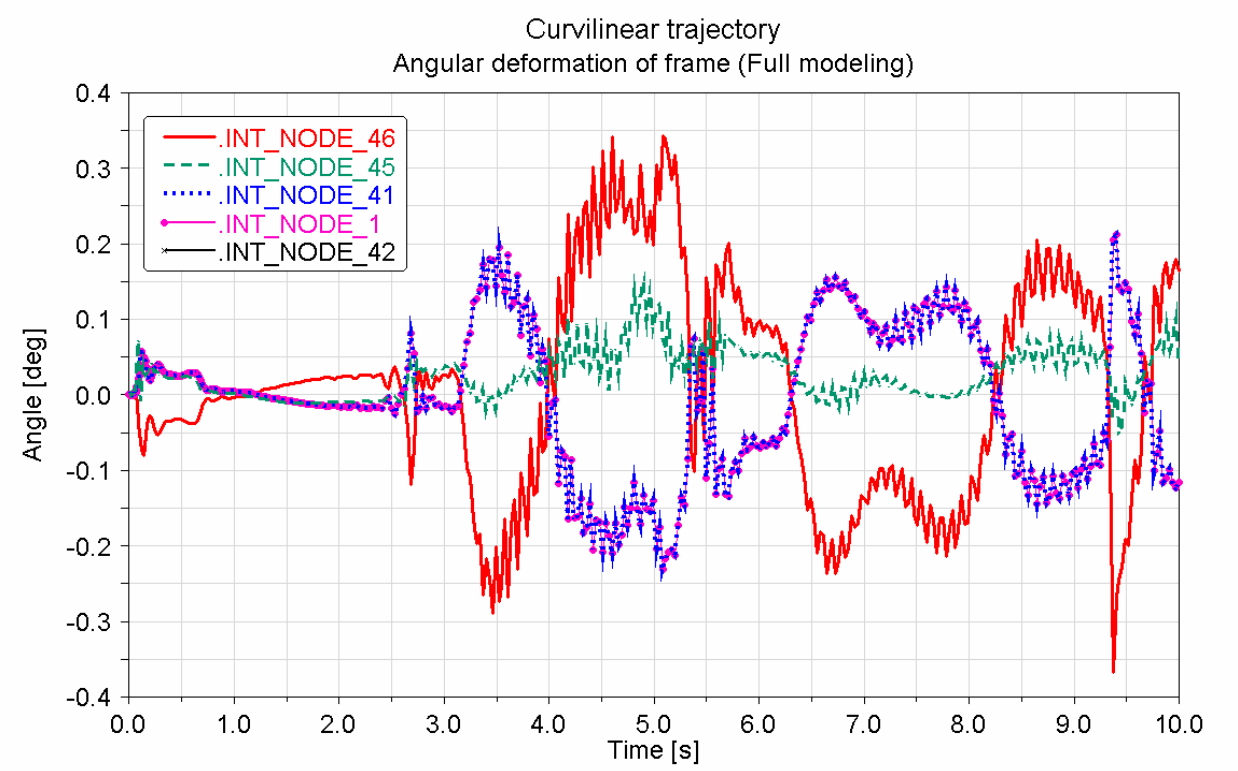

Figure 19. Relative rotation around the motorcycle x-axis

Figures 15 and 16 show the vertical components of the acceleration measured during the curvilinear trajectory at the front right engine attachment and at the rear suspension rocker arm attachment. From the graphs it is evident that again the rigid frame inertia configuration does not provide valid indications for the evaluation of handling, since in some instances the acceleration values are markedly lower than those of the other two configurations (*Full* and *Partial)* which are, instead, largely coincident.

As might be expected, the highest acceleration values are found on node 22, schematising the connection with the vibrating mass of the engine.

Figures 17 and 18 show, respectively, the flexural and torsional deformations of the frame, referring to two important points on the mid-plane of the vehicle. These measurements were made only in the case of *Full* and *Partial* inertia configurations, which in this case provide an almost coincident response, allowing an instantaneous check on the elastic-dynamic behaviour of the frame in order to validate the geometry and dimension characteristics.

Figure 19 shows the relative rotation about the vehicle's x-axis, along the direction of movement, of the points under examination.

The marker positioned near node 46, placed on the axis of the steering column sleeve, has a rotation coincident with the inclination of the motorcycle imposed by the controller in order to follow the curvilinear trajectory.

The markers corresponding to nodes 41, 1 and 42 (again approximately on the same plane, orthogonal to the vehicle's x-axis and placed at the extreme rear of the frame) initially rotate in the opposite direction because they are subjected to deformation induced by the rear wheel which, because of the gyroscopic effect, tends to right itself, opposing the inclination given by the controller.

The minimum rotation was found at the marker placed near the centre of torsion (node 45) and was determined in the *Full* inertia configuration which, as described above, provides the best response.

4. Conclusions

The study proposes a critical comparison of the results obtained using different inertia modelling techniques on a motorcycle frame. A synergetic combination of FEM and multibody programs was

used to simulate typical manoeuvres for evaluating comfort and handling performance.
In the light of the results obtained, it can be asserted that the study of motor vehicle dynamics must be conducted using flexible elements for a correct simulation of the dynamic behaviour of the frame, even though this results in more demanding calculations.
The MDI/ADAMS calculation code used allows three typologies of inertia discretisation, which differ in the weighting given to various terms of the inertia matrix: *Full*, *Partial* and *Constant*. The results obtained in both manoeuvres, passing over a hump and of following an "S" bend, evidenced very similar optimal responses when the *Full* and *Partial* inertia approaches were applied.
The flexural and torsional stiffness of the frame under examination does not allow an inertia approach of the *Constant* type. The analyses presented in this study provide the designer with important information in the pre-engineering phase. In fact there is no need to resort to prototypes and experimental trials with have the disadvantage of high costs and results often based on the subjective judgement of test riders. With this approach it is possible to fine tune the almost definitive model, reducing costs and time to market.

Acknowledgements

The authors wish to thank Dott. Ing. Simone Di Piazza and Dott. Ing. Marco Paradisi of Ducati Motor Spa for their collaboration, and Dott. Ing. Roberto Marangon of Pirelli Pneumatici Spa for the data regarding the tyres.

References

V. Cossalter, "Cinematica e dinamica della motocicletta", Edizioni Progetto, Padova, 1997.

R. S. Sharp, "The stability and control of motorcycles", Journal of Mechanical Engineering Science, Vol.13, n°5, 1971.

R. E. Roberson, R. Schwertassek, "Dynamics of Multibody Systems", Springer-Verlag, Berlino, 1988.

H. B. Pacejka, "Tyre models for Vehicle Dynamics Analisys", Swets & Zeitlenger, Amsterdam, 1991.

M. Da Lio, "Analisi della manovrabilità dei veicoli. Un approccio basato sul controllo ottimo", ATA – Ingegneria Automotoristica, n°1-2, 1997.

D. H. Weir, J. W. Zellner, "Lateral directional motorcycle dynamics and rider control", SAE 780304 Society of Automotive Engineers Inc., Warrendale, 1978.

R. E. Roberson, "On the recursive determination of body frames for multibody dynamic simulation", Journal Appl. Mechanic 52/1985.

R. Tovo, N. Facchin, "Analisi strutturale di telai motociclistici", Il Progettista Industriale Tecniche Nuove, n. 06/99.

Calì M., Garozzo A., Oliveri S.M., "Simulation of motorcycle using a multi-body numerical approach", Proceedings of the 10th ADM International Conference on Design Tools and Methods in Industrial Engineering, Firenze 17-19 Settembre 1997 (pagg.713-722).

Calì M., Manuele R., Oliveri S.M., " Analisys of the dynamic behaviour of a scooter using a three-dimensional model", Proceedings of the 11th ADM International Conference on Design Tools and Methods in Industrial Engineering, Palermo 17-19 Settembre 1997 (pagg.713-722).

Calì M., G.B Gamuzza., Oliveri S.M., "simulazione dinamica di un motoveicolo utilizzando una tecnica multibody ad elementi deformabili",Tesi di laurea, Università Degli Studi Di Catania – Facoltà di Ingegneria Anno Accademico 2000-2001.

Bradley J., "The racing motorcycle", Broadland Leisure Publications, York (England), 1996.

Prof. S.M. Oliveri
Dipartimento di Ingegneria Industriale e Meccanica, Facoltà di Ingegneria, Università di Catania
Viale Andrea Doria 6, 95124 Catania, Italia
Tel.: 095 7382404 / 095 7382412
Email: moliveri@diim.unict.it